Chapter 9
Microstrip Biomedical Patch Antenna with MIMO Capability and Challenges in Achieving Diversity Performance

Manish Sharma

Abstract The chapter discusses the microstrip patch antenna capability of transformation to $MIMO_{p\times q}$ antenna formation. A well-known fact for modern communication system needs to accommodate the higher data rate of transmission in the existing channel. The two aspects of the MIMO configuration are addressed in this chapter. The patch antenna needs to be useful for wireless communication applications and the other maintains isolation with good diversity performance evaluating ECC, DG, TARC, MEG, CCL. These are the challenges faced in designing the MIMO antenna, and the challenges are overcome in case of isolation by using different methods such as using neutralization line, using different fractals in-ground, using parasitic U-type between feed lines, placing radiating elements orthogonally, using meta-material structure, placing T-type stub in the commonly shared ground along with pair of etched comb-type slots, inverse L-type stub in the ground and interconnecting all the ground by using thin strips. These techniques provide either an additional current path between the radiating elements or by directing the current vectors in opposite direction thereby, canceling the unnecessary interference. Also, in medical applications, bandwidth of 402–405 MHz is used with power limitation of 25 W and are used in Implantation, Telemedicine applications. The ISM band of 2.45 GHz is used for detection of Skin Cancer.

Keywords MIMO · Diversity performance · Neutralization line · $ECC_{p\times q}$ · $DG_{p\times q}$ · $TARC_{p\times q}$ · $CCL_{p\times q}$ · Implantation · Telemedicine · Skin cancer

Introduction

Recent faster communication demanding the new concept of smart cities, artificial intelligence-based communication, etc. has emerged which has focused on the higher data rate transfer of information from source to destination with multiple users. However, SISO (Single–Input–Single–Output) system fulfills the requirement

M. Sharma (✉)
Chitkara University Institute of Engineering and Technology, Chitkara University, Punjab, India
e-mail: manishengineer1978@gmail.com

P. K. Malik and P. N. Shastry (eds.), *Internet of Things Enabled Antennas for Biomedical Devices and Systems*, Springer Tracts in Electrical and Electronics Engineering,
https://doi.org/10.1007/978-981-99-0212-5_9

to some extent but the operating bandwidth is compromised due to shortcomings such as multiple fading in real-time environment applications. However, the design of a microstrip MIMO antenna with smart reconfigurable technology will resolve the issues. Designing these MIMO antennas has to face lots of challenges and to name a few of them are maintaining reasonable isolation and achieving high diversity performance. The literature discussed here is an attempt to understand and overcome of above problems faced in a MIMO system. The two-port MIMO system (Tiwari et al. 2019a, b, 2020; Islam and Das 2020; Tang et al. 2020a, b; Pasumarthi et al. 2019; Wang et al. 2020; Vasu Babu and Anuradha 2019; Addepalli and Anitha 2020; Ameen et al. 2020; Hasan et al. 2019; Dkiouak et al. 2019, 2020; Hassan et al. 2020; Thakur et al. 2020; Azarm et al. 2019; Agarwal et al. 2020; Ahmed et al. 2018; Banerjee et al. 2017, 2020; Desai et al. 2022; Gupta and Kumar 2020; Gurjar et al. 2020; Mohanty and Behera 2020; Mark et al. 2019; Hadda et al. 2021; Sun et al. 2017; Sohi and Kaur 2020; Sharma et al. 2021a; Sharma 2020; Kumar et al. 2020; Oliveira et al. 2021; Kumar Biswas and Chakraborty 2019) is discussed where different methodologies have been employed for diversity performance and higher isolation between the inter-spaced elements. A neutralization line that is attached between the two adjacent radiators helps in achieving better isolation of ≤ -22 dB in the bandwidth range of 3.52–9.89 GHz (Tiwari et al. 2019a, b). Interestingly, a two-band antenna for WiMAX applications achieves isolation by etched U-shaped strip between the two feed lines (Islam and Das 2020). The two radiating elements placed face-to-face with parasitic U-type stub on opposite plane with printed stepped ground helps in achieving isolation of -15.0 dB (Tang et al. 2020a). The important technique in the form of meta-material structure is also used to obtain better isolation which is placed between the two antenna elements (Wang et al. 2020; Mark et al. 2019). Mutual coupling of more than 20 dB is achieved by using inverted L- and Ω-symbol in a 2×2 MIMO antenna (Vasu Babu and Anuradha 2019). The distance between the dual frequency bands maintains isolation of more than 15.0 dB for split-ring-resonator antennas (Ameen et al. 2020) and integrated T-type stub in ground achieves isolation of more than 21.0 dB (Tiwari et al. 2020; Tang et al. 2020b). A rectangular parasitic structure placed in ground for the orthogonally placed radiating elements is another technique to reduce isolation (Azarm et al. 2019). Addition of two rectangular strip in a CPW-fed Minkowski-fractal ground MIMO antenna improves isolation from 14.71 to 21.81 dB (Banerjee et al. 2017) and using Hilbert-fractal in ground also increases level of isolation (Banerjee et al. 2020; Gurjar et al. 2020). Also, in dual notched band UWB-MIMO antenna, isolation is achieved without using any decoupling element and placement of dual radiators at 90° to each other offers nil interaction between them (Hadda et al. 2021; Sharma et al. 2021a). 2-port $\text{MIMO}_{\text{p}\times\text{q}}$ with embedded T-type stub sharing commonly ground provides sufficient isolation to achieve permissible diversity performance (Sharma 2020; Kumar et al. 2020). The shape of integer "8" is used in the middle of ground providing better isolation and the designed antenna is useful for wearable applications (Kumar Biswas and Chakraborty 2019).

The reported literature also discusses four-port MIMO antenna configuration (Dhasarathan et al. 2020; Yussuf and Paker 2019; Srivastava et al. 2019a, b; Roy

et al. 2021; Bactavatchalame and Rajakani 2020; Sharma et al. 2020a, b, 2021b; Raheja et al. 2019, 2020; Khan et al. 2020; Mohammad Saadh et al. 2020; McHbal et al. 2020; Andrade-González et al. 2021; Sehrai et al. 2021; Agarwal et al. 2021; Hussain et al. 2022; Ali et al. 2021; Hassan et al. 2019; Arumugam et al. 2021; Khandelwal 2020; Mathur and Dwari 2018; Pahadsingh and Sahu 2018; Mohanty and Sahu 2021; Prabhu and Malarvizhi 2019; Singh et al. 2021; Fritz-Andrade et al. 2019) where different techniques are used to achieve higher isolation. In 4 × 4 hexagonal shape MIMO antenna with isolated ground, observes no decoupling structure for better isolation but the arrangement of all the four antennas is such that the radiated signal will not interfere (Dhasarathan et al. 2020). The mutual coupling in the 4 × 4 MIMO antenna is achieved by using a cross-shaped stub between the four radiators for improvement of the isolation (Yussuf and Paker 2019). An integrated Bluetooth UWB antenna arranged in orthogonal sequence needs no decoupling element to achieve better isolation (Srivastava et al. 2019a; Sharma et al. 2020a, b, 2021b; Mohammad Saadh et al. 2020; Sehrai et al. 2021; Ali et al. 2021; Arumugam et al. 2021; Raheja et al. 2020; Addepalli et al. 2022) and by using isolated meander line above the common-shared ground enhances the port-to-port isolation (Roy et al. 2021). Also, Electro-magnetic Band Gap Structure is used to achieve isolation which is also one of the prominent techniques in achieving isolation (Prabhu and Malarvizhi 2019). The literature work presented over here also discusses 6- and 8-port MIMO antenna configuration (Chung and Hsiao 2022; Mathur and Dwari 2019; Biswal and Das 2019) and utilizes various mechanisms to achieve higher isolation between the inter-element radiators. The 8 × 8 $\text{MIMO}_{p\times q}$ targeted for Ultra-WB usage utilizes 8-etched slits in-ground providing higher isolation (Mathur and Dwari 2019) and common-shared ground with eight radiators providing resonance at 5.50 GHz uses no additional isolation structure (Biswal and Das 2019). A significant review is conducted on chronic diseases involving instruments like MRI, X-Ray, mammography, ultrasound and different diagnosed diseases. The antennas are useful in telemedicine applications at frequency centered at 2.45 GHz (Arora et al. 2021). The skin model represented in Shreshtha et al. (2021) utilizes antenna with resonance of 2.45 GHz (Tiwari and Malik 2020; Gupta et al. 2020; Roges et al. 2022).

Two and Four-Port MIMO Antennas

The configuration of the 2- and 4-port MIMO antenna is depicted in Fig. 9.1. Figure 9.1a represents a 2-port MIMO antenna with a compact size of 21 × 34 × 1.6 mm^3. In this reported work (Tiwari et al. 2019a), FR4 substrate is used with a constant-dielectric value of 4.40 and a tangent (β) = 0.02 with a height of 1.60 mm. The width of the feed is 2.24 mm which corresponds to a matching of 50 Ω impedance. Introduction of a neutralization line between the two radiating elements offers a bandwidth of 3.53–9.91 GHz and maintains isolation of ≤ -22.0 dB. The surface current distribution over the surface is carried out at 3.53 and 9.91 GHz, respectively, as shown in Fig. 9.1c, d. It can be derived that the direction of the current flow in

the neutralization line and mid-ground are opposite to each other, thus canceling the interfering field which reduces the interference. This neutralization technique employed in the 2 × 2 MIMO antenna improves the matching of the impedance in the operating band and thus, improved S-parameters (S_{11}, S_{12}, S_{21}, S_{22}) are obtained. This MIMO antenna is useful in different wireless applications including HiperLAN operating between 5.00 and 6.00 GHz, maritime applications for different bands, and WLAN, WiMAX, and ISM bands. On the other hand, the diversity performance parameters include ECC to be 0.05 correspondingly Directive Gain is approximately 10.0 dB with CCL $\leq$ 0.26 bits/s/Hz (Tiwari et al. 2019a).

A four-port (Ali et al. 2021) MIMO antenna produces a single resonant frequency for a 5G n78/79 communication system. The designed four-port MIMO antenna is instrumental in hand-held 5G devices application with the compact size of 40 × 40 mm^2 and hence, shows the Specific-Absorption-Rate (SAR) value of 0.90 W/Kg and offers channel capacity of data transmission to be 18.7 bps/Hz. The single-element version is fabricated on an FR4 substrate with an overall size of 20 × 20 mm^2. The antenna or radiator is printed on one plane of the substrate which looks like an inverted L-type patch, and the opposite plane is printed with ground dimensions of 20 × 20 mm^2 with an etched rectangular slot below the radiating patch. This configuration of the antenna provides a narrow bandwidth with a center resonating frequency of 4.79 GHz. The S_{11}/S_{22} shows the resonant frequency centered at 4.85 and 4.82 GHz. This configuration of the $MIMO_{p\times q}$ antenna is intended to providing pattern diversity with maximum lobe directed at 280° for Ant. 1 and 208° for Ant. 3. Ant. 2 corresponds to the maximum gain lobe between 90° and 120° and opposite values of −90° to −120° for Ant. 4 (Ali et al. 2021).

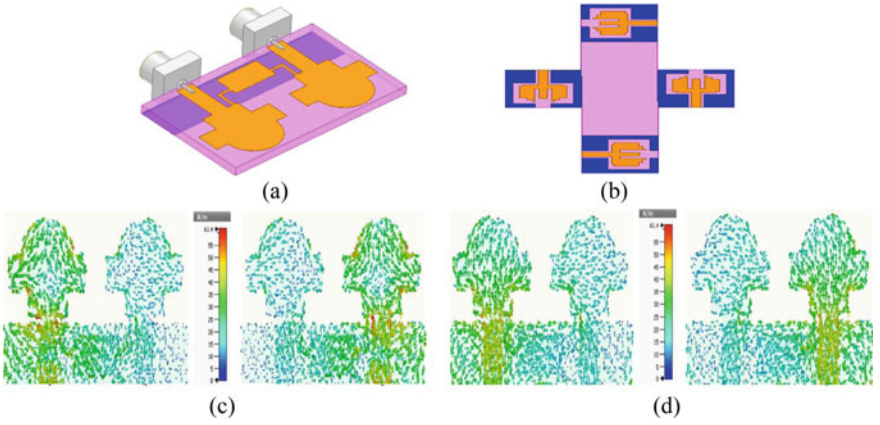

Fig. 9.1 MIMO configuration **a** 2-port with neutralization line (Tiwari et al. 2019a) **b** 4-port MIMO antenna (Mohammad Saadh et al. 2020) (**a**), (**b**) 3.53 GHz and 9.91 GHz (Tiwari et al. 2019a)

Understanding Eight-Port MIMO Antenna

A case study (Addepalli et al. 2022) is used to explain the working principle of an 8-port MIMO antenna. Figure 9.2 shows the single-element antenna configuration with a printed patch on one plane and ground on opposite plane of FR4 substrate. Figure 9.2 also illustrates the flower-shaped radiating patch with five leaves shaped stubs embedded in the semi-circular patch. The partial ground with a height of 13.50 mm is etched with a semi-elliptical slot placed below the microstrip for better matching of the impedance. Also, as per the observations from Fig. 9.2, two rectangular stubs and a pair of rotated L-strips are placed which act as reflectors and direct the signal in the direction of radiation.

Figure 9.3a, b shows the four-port configuration with a perspective view and transparent front view. Firstly, the substrate with an area of $D_1 \times D_2$ mm^2 is removed from all the four corners within the substrate of the dimension of $D_L \times D_W$ mm^2. The four-radiating patch is placed in an orthogonal fashion with their respective ground. Lastly, a square patch of dimension $D_5 \times D_6$ mm^2 is placed exactly at the center containing ground, and all the four ground are connected to the centrally placed patch by a rectangular strip of dimension $(D_2 + D_3 + D_4)$ mm. This ground modification is carried out to achieve higher isolation between the inter-spaced elements. The S_{11} parameter of the four-port transformed MIMO antenna is compared with the single-element antenna shown in Fig. 9.3c and can be concluded that the required impedance bandwidth for 5G-n77/78 band is achieved in both the cases with very good resonance at the center frequency. Figure 9.3c shows the isolation of Port 1 concerning Port 2, Port 3, and Port 4 providing isolation of more than 15.0 dB.

Finally, Fig. 9.4 shows an 8-port MIMO antenna with a fabricated prototype shown in Fig. 9.4a (Front + Ground), and Fig. 9.4b shows the simulation environment. As per the observations from Fig. 9.4a, b, eight radiating elements are used on the FR4 substrate with a total area of 2.147λg × 2.147 λg mm^2. It can be seen that the A_1/A_5,

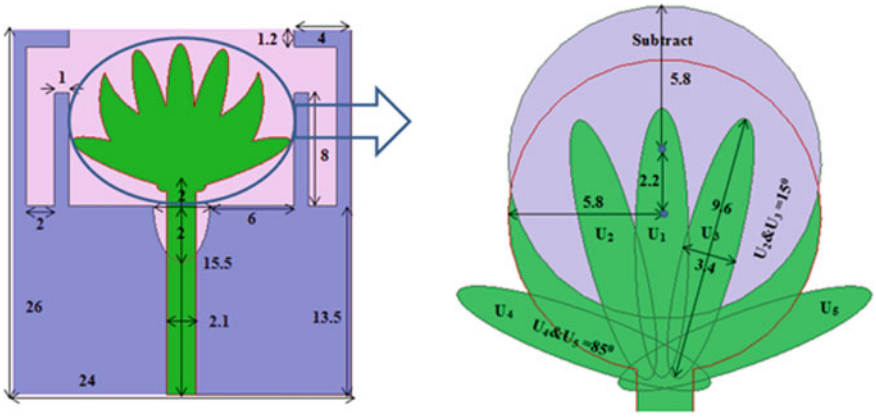

Fig. 9.2 Configuration of the single-element antenna (Addepalli et al. 2022)

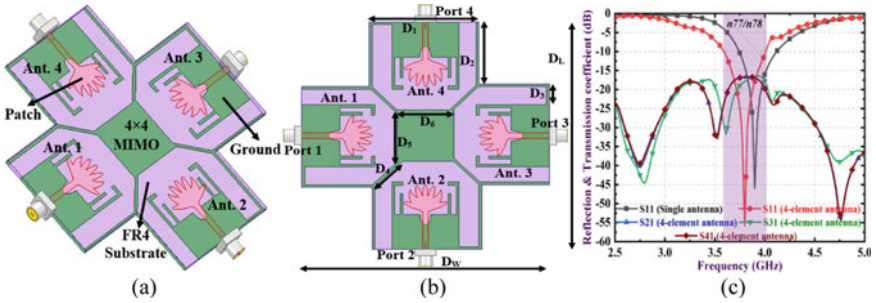

Fig. 9.3 Four port MIMO antenna **a** perspective view **b** transparent front view **c** reflection and transmission coefficients (Addepalli et al. 2022)

A_2/A_6, A_3/A_7, and A_4/A_8 are placed adjacent to each other with a spacing of 13.50 mm while all the four pairs are placed orthogonally. The ground of all the eight antennas is connected by rectangular strips with a dimension of 81.0 mm to the rectangle patch of dimension 30 × 30 mm^2 in the ground plane for better isolation. Figure 9.4c shows the comparison of the S_{11} parameter of all the three antennas discussed (Single-, Four-, and Eight-port) with all the three versions covering 5G-n77/n78 bands.

Figure 9.4d shows the measured reflection and transmission coefficients. It can be observed that the reflection coefficients $S_{11}/S_{22}/S_{33}/S_{44}$ are overlapped with each other in the 5G-n77/78 band with good impedance matching and the transmission coefficients of Port 1 concerning Port 2. Port 3, Port 4, Port 5, Port 6, Port 7, and Port 8 offers isolation of more than 20.0 dB.

Conclusions

The challenge in designing MIMO antenna configuration with two-, four-, and Eight-port was discussed. It was concluded that the few MIMO antennae with orthogonal placed required no additional isolation element to avoid the interference making the design simple. However, techniques such as neutralization line, which commonly connected ground by using thin rectangular stubs in-ground resulted in higher isolation between the closely placed radiating elements. It was also concluded that by maintaining isolation of more than 10 dB, the impedance bandwidth of all the individual radiating elements of the MIMO antenna was preserved without any deterioration.

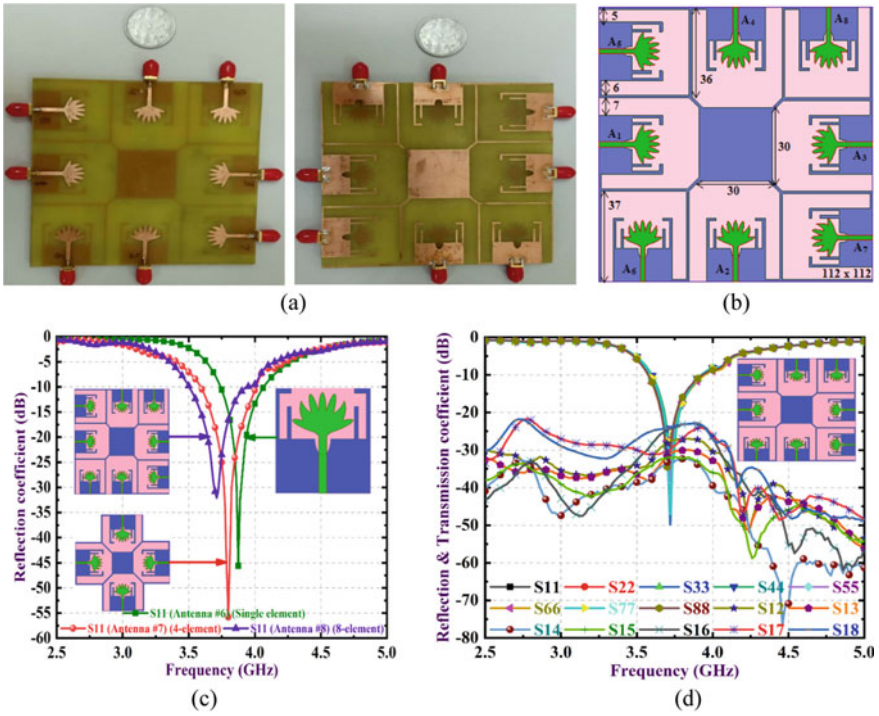

Fig. 9.4 Eight-port MIMO antenna **a** photograph of eight-port MIMO antenna (front + ground) **b** simulation environment **c** comparison of S-parameter (single-, four-, and eight-port MIMO antenna) **d** reflection and Transmission coefficients (Addepalli et al. 2022)

References

Addepalli T, Anitha VR (2020) A very compact and closely spaced circular shaped UWB MIMO antenna with improved isolation. AEU Int J Electron Commun 114

Addepalli T, Kamili JB, Bandi KK, Nella A, Sharma M (2022) Lotus flower-shaped 4/8-element MIMO antenna for 5G n77 and n78 band applications. J Electromagn Waves Appl. https://doi.org/10.1080/09205071.2022.2028683

Agarwal M, Dhanoa JK, Khandelwal MK (2020) Ultrawide band two-port MIMO diversity antenna with triple notch bands, stable gain and suppressed mutual coupling. AEU Int J Electron Commun 120

Agarwal S, Rafique U, Ullah R, Ullah S, Khan S, Donelli M (2021) Double overt-leaf shaped CPW-fed four port UWB MIMO antenna. Electronics 10(24)

Ahmed BT, Olivares PS, Campos JLM, Vázquez FM (2018) (3.1–20) GHz MIMO antennas. AEU-Int J Electron C 94:348–358

Ali H et al (2021) Four-port MIMO antenna system for 5G n79 band RF devices. Electronics 11(1)

Ameen M, Ahmad O, Chaudhary RK (2020) Single split-ring resonator loaded self-decoupled dual-polarized MIMO antenna for mid-band 5G and C-band applications. AEU Int J Electron Commun 124

Andrade-González EA, Tirado-Méndez JA, Jardón-Aguilar H, Reyes-Ayala M, Rangel-Merino A, Pascoe-Chalke M (2021) UWB four ports MIMO antenna based on inscribed Fibonacci circles. J Electromagn Waves Appl 35(9):1202–1220

Arora G, Maman P, Sharma A, Verma N, Puri V (2021) Systematic overview of microstrip patch antenna's for different biomedical applications. Adv Pharm Bull 11(3):439–449

Arumugam S, Manoharan S, Palaniswamy SK, Kumar S (2021) Design and performance analysis of a compact quad-element UWB MIMO antenna for automotive communications. Electronics 10(18)

Azarm B, Nourinia J, Ghobadi C, Majidzadeh M, Hatami N (2019) On development of a MIMO antenna for coupling reduction and WiMAX suppression purposes. AEU-Int J Electron C 99:226–235

Bactavatchalame P, Rajakani K (2020) Compact broadband slot-based MIMO antenna array for vehicular environment. Microw Opt Technol Lett 62(5):2024–2032

Banerjee J, Karmakar A, Ghatak R, Poddar DR (2017) Compact CPW-fed UWB MIMO antenna with a novel modified Minkowski fractal defected ground structure (DGS) for high isolation and triple band-notch characteristic. J Electromagn Waves Appl 31(15):1550–1565

Banerjee J, Gorai A, Ghatak R (2020) Design and analysis of a compact UWB MIMO antenna incorporating fractal inspired isolation improvement and band rejection structures. AEU Int J Electron Commun 122

Biswal SP, Das S (2019) Eight-element-based MIMO antenna with CP behaviour for modern wireless communication. IET Microw Antennas Propag 14(1):45–52

Chung M-A, Hsiao C-W (2022) Dual-band 6 × 6 MIMO antenna system for glasses applications compatible with Wi-Fi 6E and 7 wireless communication standards. Electronics 11(5)

Desai A et al (2022) Transparent 2-element 5G MIMO antenna for sub-6 GHz applications. Electronics 11(2)

Dhasarathan V, Nguyen TK, Sharma M, Patel SK, Mittal SK, Pandian MT (2020) Design, analysis and characterization of four port multiple-input-multiple-output UWB-X band antenna with band rejection ability for wireless network applications. Wirel Netw 26(6):4287–4302

Dkiouak A, Zakriti A, El Ouahabi M (2019) Design of a compact dual-band MIMO antenna with high isolation for WLAN and X-band satellite by using orthogonal polarization. J Electromagn Waves Appl 34(9):1254–1267

Dkiouak A, Zakriti A, El Ouahabi M, McHbal A (2020) Design of two element Wi-MAX/WLAN MIMO antenna with improved isolation using a short stub-loaded resonator (SSLR). J Electromagn Waves Appl 34(9):1268–1282

Fritz-Andrade E, Perez-Miguel A, Gomez-Villanueva R, Jardon-Aguilar H (2019) Characteristic mode analysis applied to reduce the mutual coupling of a four-element patch MIMO antenna using a defected ground structure. IET Microw Antennas Propag 14(2):215–226

Gupta A, Kumar V (2020) DGS-based wideband MIMO antenna for on–off body communication with port isolation enhancement operating at 2.45 GHz industrial scientific and medical band. J Electromagn Waves Appl 35(7):888–901

Gupta NP, Malik PK, Ram BS (2020) A review on methods and systems for early breast cancer detection. In: 2020 International conference on computation, automation and knowledge management (ICCAKM), pp 42–46. https://doi.org/10.1109/ICCAKM46823.2020.9051554. ISBN: 978-1-7281-0666-3. https://ieeexplore.ieee.org/document/9051554

Gurjar R, Upadhyay DK, Kanaujia BK, Kumar A (2020) A compact modified sierpinski carpet fractal UWB MIMO antenna with square-shaped funnel-like ground stub. AEU Int J Electron Commun 117

Hadda L, Sharma M, Gupta N, Kumar S, Singh AK (2021) On-demand reconfigurable WiMAX/WLAN UWB-X band high isolation 2×2 MIMO antenna for imaging applications. IETE J Res 1–13

Hasan MN, Bashir S, Chu S (2019) Dual band omnidirectional millimeter wave antenna for 5G communications. J Electromagn Waves Appl 33(12):1581–1590

Hassan MM et al (2019) A novel UWB MIMO antenna array with band notch characteristics using parasitic decoupler. J Electromagn Waves Appl 34(9):1225–1238
Hassan MM et al (2020) Two element MIMO antenna with frequency reconfigurable characteristics utilizing RF MEMS for 5G applications. J Electromagn Waves Appl 34(9):1210–1224
Hussain M et al (2022) Design and characterization of compact broadband antenna and its MIMO configuration for 28 GHz 5G applications. Electronics 11(4)
Islam SN, Das S (2020) Dual-band CPW fed MIMO antenna with polarization diversity and improved gain. Int J RF Microw Comput-Aided Eng 30(4)
Khan MS, Naqvi SA, Iftikhar A, Asif SM, Fida A, Shubair RM (2020) A WLAN band-notched compact four element UWB MIMO antenna. Int J RF Microw Comput-Aided Eng 30(9)
Khandelwal MK (2020) Metamaterial based circularly polarized four-port MIMO diversity antenna embedded with slow-wave structure for miniaturization and suppression of mutual coupling. AEU Int J Electron Commun 121
Kumar Biswas A, Chakraborty U (2019) Compact wearable MIMO antenna with improved port isolation for ultra-wideband applications. IET Microw Antennas Propag 13(4):498–504
Kumar A, Ansari AQ, Kanaujia BK, Kishor J, Kumar S (2020) An ultra-compact two-port UWB-MIMO antenna with dual band-notched characteristics. AEU Int J Electron Commun 114
Mark R, Rajak N, Mandal K, Das S (2019) Metamaterial based superstrate towards the isolation and gain enhancement of MIMO antenna for WLAN application. AEU-Int J Electron C 100:144–152
Mathur R, Dwari S (2018) Compact CPW-fed ultrawideband MIMO antenna using hexagonal ring monopole antenna elements. AEU-Int J Electron C 93:1–6
Mathur R, Dwari S (2019) 8-port multibeam planar UWB-MIMO antenna with pattern and polarisation diversity. IET Microw Antennas Propag 13(13):2297–2302
McHbal A, Amar Touhami N, Elftouh H, Dkiouak A (2020) Coupling reduction using a novel circular ripple-shaped decoupling mechanism in a four-element UWB MIMO antenna design. J Electromagn Waves Appl 34(12):1647–1666
Mohammad Saadh AW, Ashwath K, Ramaswamy P, Ali T, Anguera J (2020) A uniquely shaped MIMO antenna on FR4 material to enhance isolation and bandwidth for wireless applications. AEU Int J Electron Commun 123
Mohanty A, Behera BR (2020) Investigation of 2-port UWB MIMO diversity antenna design using characteristics mode analysis. AEU Int J Electron Commun 124
Mohanty A, Sahu S (2021) Integration of coupling resonator as port-isolator and MMLC-Minkowiski fractal loop for Wi-Max rejection in 4-port compact UWB MIMO antenna. J Electromagn Waves Appl 35(10):1359–1377
Oliveira JGD, D'Assunção Junior AG, Silva Neto VP, D'Assunção AG (2021) New compact MIMO antenna for 5G, WiMAX and WLAN technologies with dual polarisation and element diversity. IET Microw Antennas Propag 15(4):415–426
Pahadsingh S, Sahu S (2018) Four port MIMO integrated antenna system with DRA for cognitive radio platforms. AEU-Int J Electron C 92:98–110
Pasumarthi SR, Kamili JB, Avala MP (2019) Design of dual band MIMO antenna with improved isolation. Microw Opt Technol Lett 61(6):1579–1583
Prabhu P, Malarvizhi S (2019) Novel double-side EBG based mutual coupling reduction for compact quad port UWB MIMO antenna. AEU-Int J Electron C 109:146–156
Raheja DK, Kanaujia BK, Kumar S (2019) Compact four-port MIMO antenna on slotted-edge substrate with dual-band rejection characteristics. Int J RF Microw Comput-Aided Eng 29(7)
Raheja DK, Kumar S, Kanaujia BK (2020) Compact quasi-elliptical-self-complementary four-port super-wideband MIMO antenna with dual band elimination characteristics. AEU Int J Electron Commun 114
Roges R, Malik PK, Sharma S (2022) A compact wideband antenna with DGS for IoT applications using LoRa technology. In: 2022 10th International conference on emerging trends in engineering and technology—signal and information processing (ICETET-SIP-22), pp 1–4. https://doi.org/10.1109/ICETET-SIP-2254415.2022.9791725

Roy S, Biswas AK, Ghosh S, Chakraborty U, Sarkhel A (2021) Isolation improvement of dual-/quad-element textile MIMO antenna for 5G application. J Electromagn Waves Appl 35(10):1337–1353
Sehrai DA et al (2021) Compact quad-element high-isolation wideband MIMO antenna for mm-wave applications. Electronics 10(11)
Sharma M (2020) Design and analysis of MIMO antenna with high isolation and dual notched band characteristics for wireless applications. Wirel Pers Commun 112(3):1587–1599
Sharma M, Dhasarathan V, Patel SK, Nguyen TK (2020a) An ultra-compact four-port 4 × 4 super-wideband MIMO antenna including mitigation of dual notched bands characteristics designed for wireless network applications. AEU Int J Electron Commun 123
Sharma M, Vashist PC, Ashtankar PS, Mittal SK (2020b) Compact 2 × 2/4 × 4 tapered microstrip feed MIMO antenna configuration for high-speed wireless applications with band stop filters. Int J RF Microw Comput-Aided Eng 31(1)
Sharma M, Kumar R, Kaur P, Dhasarathan V, Nguyen TK (2021a) Design and analysis of on-demand reconfigurable WiMAX/WLAN high isolation 2 × 2 MIMO antenna oriented adjacent/orthogonally for imaging applications in UWB-X band. Int J RF Microw Comput-Aided Eng 32(1)
Sharma M, Vashist PC, Alsukayti I, Goyal N, Anand D, Mosavi AH (2021b) A wider impedance bandwidth dual filter symmetrical MIMO antenna for high-speed wideband wireless applications. Symmetry 14(1)
Shreshtha S, Aggarwal M, Ghane P, Varahramyan K (2021) Flexible microstrip antenna for skin contact application. Int J Antennas Propag Article ID 745426:1–6. https://doi.org/10.1155/2012/745426
Singh D et al (2021) Inverted-c ground MIMO antenna for compact UWB applications. J Electromagn Waves Appl 35(15):2078–2091
Sohi AK, Kaur A (2020) Hexa-band suppression characteristics from a fork-shaped UWB-MIMO antenna loaded with complementary split-ring resonator and slots. J Electromagn Waves Appl 34(16):2194–2219
Srivastava K, Kumar A, Kanaujia BK, Dwari S, Kumar S (2019a) A CPW-fed UWB MIMO antenna with integrated GSM band and dual band notches. Int J RF Microw Comput-Aided Eng 29(1)
Srivastava K, Kanaujia BK, Dwari S, Kumar S, Khan T (2019b) 3D cuboidal design MIMO/diversity antenna with band notched characteristics. AEU-Int J Electron C 108:141–147
Sun D, Wang P, Gao P, Zhang Y (2017) A novel dual-band MIMO antenna with two rings for WIMAX applications. J Electromagn Waves Appl 32(3):274–280
Tang X, Yao Z, Li Y, Zong W, Liu G, Shan F (2020a) A high performance UWB MIMO antenna with defected ground structure and U-shape branches. Int J RF Microw Comput-Aided Eng 31(2)
Tang Z, Zhan J, Wu X, Xi Z, Chen L, Hu S (2020b) Design of a compact UWB-MIMO antenna with high isolation and dual band-notched characteristics. J Electromagn Waves Appl 34(4):500–513
Thakur E, Jaglan N, Gupta SD (2020) Design of compact triple band-notched UWB MIMO antenna with TVC-EBG structure. J Electromagn Waves Appl 34(11):1601–1615
Tiwari P, Malik PK (2020) Design of UWB antenna for the 5G mobile communication applications: a review. In: 2020 International conference on computation, automation and knowledge management (ICCAKM), pp 24–30. https://doi.org/10.1109/ICCAKM46823.2020.9051556. ISBN: 978-1-7281-0666-3. https://ieeexplore.ieee.org/document/9051556
Tiwari RN, Singh P, Kanaujia BK (2019a) A compact UWB MIMO antenna with neutralization line for WLAN/ISM/mobile applications. Int J RF Microw Comput-Aided Eng 29(11)
Tiwari RN, Singh P, Kanaujia BK, Srivastava K (2019b) Neutralization technique based two and four port high isolation MIMO antennas for UWB communication. AEU Int J Electron Commun 110
Tiwari RN, Singh P, Kanaujia BK, Kumar S, Gupta SK (2020) A low profile dual band MIMO antenna for LTE/Bluetooth/Wi-Fi/WLAN applications. J Electromagn Waves Appl 34(9):1239–1253
Vasu Babu K, Anuradha B (2019) Design of inverted L-shape & ohm symbol inserted MIMO antenna to reduce the mutual coupling. AEU Int J Electron Commun 105:42–53

Wang C, Yang XS, Wang BZ (2020) A metamaterial-based compact broadband planar monopole MIMO antenna with high isolation. Microw Opt Technol Lett 62(9):2965–2970
Yussuf AA, Paker S (2019) Design of a compact quad-radiating element MIMO antenna for LTE/Wi-Fi application. AEU Int J Electron Commun 111